Progress In Electromagnetics Research M, Vol. 40, 167–178, 2014

Effects of Electromagnetic Disturbance on Light Intensity Signal of Laser Beam System

Han-Chang Tsai*

Abstract—In performing the experiments, the interference source has the form of a hollow PVC tube wrapped with a current-carrying coil, while the detector has the form of a PIN (Positive-Intrinsic-Negative) photodiode. The experimental results show that the electromagnetic disturbance (EMD) signal effect is dependent on the number of turns, the direction of the electromagnetic field, and the frequency and amplitude of the interference voltage. Specifically, it is shown that when the electromagnetic field acts in the opposite direction to that of the laser beam, the intensity and optical power of the detected signal decrease with an increasing interference frequency or amplitude. By contrast, when the electromagnetic field acts in the same direction as that of the laser beam, the intensity and optical power increase with an increasing interference frequency or amplitude. In addition, it is shown that the effect of EMD on the intensity of the laser beam increases with an increasing laser beam dispersion (i.e., an increasing distance from the laser source).

1. INTRODUCTION

The proliferation of electronic and wireless devices in recent decades has brought about remarkable benefits, such as greater connectivity, improved efficiency, a more convenient lifestyle, and so on. However, it has also given rise to the problem of electromagnetic interference (EMI) [1–16], in which the desired signals of an electronic device are interfered with by the electromagnetic field generated by another device. In most cases, the effects of EMI are no more than a mere annoyance, e.g., aircraft, hospitals, implanted cardiac devices, and so on, EMI can have potentially disastrous effects. As the complexity of the electronic circuits used in modern devices continues to increase, the problem of EMI becomes increasingly severe. Thus, exploring the origins and effects of EMI, and devising effective means of shielding electronic devices from these effects, is a matter of great concern in the electronics and wireless communications fields. This experiment contains signal emitter, transmission and receiver already have the basic elements of the communication system, which uses electromagnetic wave of a current-carrying coil (it is also an inductance) to interfere the laser light signal and study how many photons is affected, it is a very specific aspect of interference: the interaction between the magnetic field and the laser beam.

The present study considers the particular case of an inductance generating an electromagnetic wave on the light intensity signal of a laser system with a central wavelength of 532 nm. Laser systems with such operating wavelengths are common in such applications as in life, education, medicine, and other military laser equipment. Consequently, the effects of EMD on their operation are an important concern.

Most electrical home appliances emit electromagnetic radiation in the low frequency range. Accordingly, the present study considers EMD with a frequency of 100 Hz∼1 kHz and an amplitude of 0∼0.6 V. The results show that the effects of EMD increases with an increasing interference frequency

Received 13 November 2014, Accepted 18 December 2014, Scheduled 7 January 2015
* Corresponding author: Han-Chang Tsai (hctsai@csu.edu.tw).
The author is with the Department of Electronic Engineering, Chen-Shiu University, Taiwan, R.O.C.

or amplitude and an increasing dispersion of the laser beam. In general, the findings presented in this study provide a useful source of information for circuit designers, laser metrology design engineers, and others in the environmental, electrical and electronics fields.

2. EXPERIMENTS

Figure 1 presents a schematic illustration of the experimental setup used in the present study. As shown, the main items of equipment include a pulsed laser source (green optical emitter, wavelength 532 nm, a frequency of 100 Hz, GLM-L1PB-05a), two interference sources (PVC plastic tubes wrapped with a current-carrying coil), and a PIN (Positive-Intrinsic-Negative) photodiode (THORLABS DET110). In performing the experiments, the photodetector was interfaced to a signal analysis and measurement system comprising an HP oscilloscope (Model 54610B) and an Agilent spectrum analyzer (Model E4440A, 3 Hz∼26.5 GHz). To highlight the effect of EMD, the experimental system use attenuator to reduce the laser light intensity. Finally, the entire system was operated under the control of a PC fitted with a GPIB interface card and LabVIEW software.

In performing optical measurement experiments, any external light sources should be isolated due to the high sensitivity of the photodetector [17–19]. Thus, this study must turn off the interior lights when the experiment. Furthermore, the various items of equipment were fixed securely in place in order to minimize experimental noise caused by changes in the angle, distance or direction of the laser beam.

3. THEORETICAL ANALYSIS

In the setup shown in Figure 1, the laser beam was passed though Interference Source I (IS 1), reflected by a mirror, passed through IS 2, and was then incident on the PIN detector. The interfered light signal was then transmitted to the oscilloscope and spectrum analyzer in order to obtain the time domain spectrum of the detected light signal. In performing the experiments, a pulse voltage ($V_p = 0 \sim 0.6$ V,

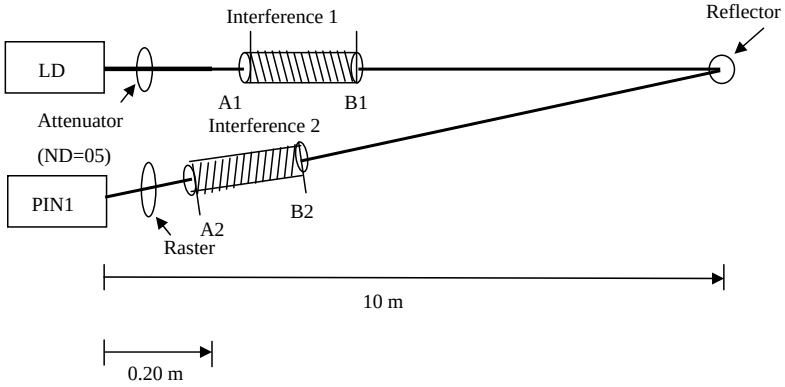

Figure 1. Experimental setup for EMD spectrum measurement.

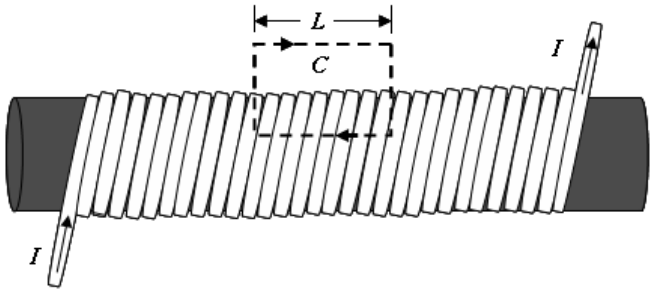

Figure 2. PVC tube wrapped with current-carrying coil.

$f = 500\,\text{Hz}$) and periodic square wave (100 Hz to 1 kHz, $V_p = 0.4\,\text{V}$) were applied in various combinations and directions across points A1 and B1 of IS 1 and A2 and B2 of IS 2. The effects of the resulting EMD on the laser signal were then investigated by examining the corresponding output voltage waveform and interference noise spectrum.

3.1. Magnetic Interference

The Lorentz force (F) acting on a charge q moves with velocity v in the presence of both a magnetic field B and an electric field E, it is given by

$$\vec{F} = q\vec{E} + q\vec{v} \times \vec{B}, \tag{1}$$

Figure 2 presents a schematic illustration of the interference sources used in the present study, comprising a current-carrying coil wrapped around a hollow PVC tube. Let the current carried by the coil be denoted as I and assume that the coil is wrapped with N turns per unit length. In accordance with Ampere's circuit law, the current passing through the coil induces a magnetic field in a direction given by Ampere's right-hand rule. Consider a rectangular path C, and assume that the tube is tightly wrapped such that the magnetic field is parallel to the tube axis. From Ampere's circuit law, the intensity (B) of the induced magnetic field is given as [20]

$$B = \mu_0 NI, \tag{2}$$

where μ_0 is the permeability of free space.

As shown in Equation (2), B depends only on the number of loops per unit length (N) and the magnitude of the current passing through the coil (I). Note that N and I have values of 500 turns and 0∼0.019 A, respectively, in the present study. The magnetic field density and flux density at the end of the solenoid are given respectively as [21]

$$H = \mu_0 B, \tag{3}$$

$$P_r = \frac{1}{2}\int \mu_0 H^2 dv = \frac{1}{2}\int HB dv. \tag{4}$$

Note that P_r represents the average energy per second at the end of the solenoid. By the Equations (2) and (4) in terms of the experimental $V_P = 0.25\,\text{V}$ and $V_P = 0.3\,\text{V}$, obtaining the P_r value are 53.18 mW and 76.93 mW, respectively. It is shown the value of the difference is $\Delta P_r = 23.75\,\text{mW}$, and which corresponds to impact the number of photons seen from Table 1 for 0.295E12.

Table 1. Effect of reverse pulse amplitude interference V_{P1} on laser beam voltage, optical power and photon number.

Interference amplitude (V_{P1})	V_{rms}	Optical power P_{PIN}	$\Delta P_{\text{PIN}} = P_x - P_{\text{NI}}$	Number of photons/sec
No interference (NI)	4.664 V	8.33 μW	0 μW	0
0.05 V	3.934 V	8.24 μW	0.09 μW	2.409E11
0.1 V	3.77 V	8.16 μW	0.17 μW	4.550E11
0.15 V	3.715 V	8.08 μW	0.25 μW	6.691E11
0.2 V	3.642 V	7.93 μW	0.40 μW	1.071E12
0.25 V	3.574 V	7.75 μW	0.58 μW	1.552E12
0.3 V	3.505 V	7.64 μW	0.69 μW	1.847E12
0.35 V	3.417 V	7.53 μW	0.80 μW	2.141E12
0.4 V	3.372 V	7.43 μW	0.90 μW	2.409E12
0.45 V	3.348 V	7.33 μW	1.00 μW	2.676E12
0.5 V	3.263 V	7.25 μW	1.08 μW	2.890E12
0.55 V	3.213 V	7.1 μW	1.23 μW	3.292E12
0.6 V	3.137 V	7.05 μW	1.28 μW	3.426E12

3.2. Quantum Particles

Einstein suggested that the energy of a light beam is not spread evenly but is concentrated in certain regions, which propagate like particles known as "photons". Einstein was led to the concept of photons by the work of Planck on the emission of light from hot bodies. Planck found that light energy is emitted in multiples of a certain minimum energy unit. The size of this energy unit, referred to as a quantum, depends on the wavelength λ of the radiation and is given by [22]

$$E = \frac{hc}{\lambda} = hf. \tag{5}$$

where h is Planck's constant, c is the light velocity, λ is the light wavelength, and f is the light frequency. For the laser beam considered in the present study, the wavelength is equal to 532 nm and the frequency is equal to 5.639E14 Hz. Thus, the photon energy is equal to 3.736E-19 J.

In the present experiments, the effects of EMD on the laser beam intensity was evaluated given two different directions of the magnetic field in the interference sources, namely (1) the reverse direction (i.e., in the opposite direction to that of the laser beam), and (2) the forward direction (i.e., in the same direction as the laser beam). Intuitively, the magnetic field in the former case impedes the forward scattering of the photons, and therefore reduces the light intensity. By contrast, in the latter case, the forward scattering of the photons in enhanced, and hence the light intensity increases.

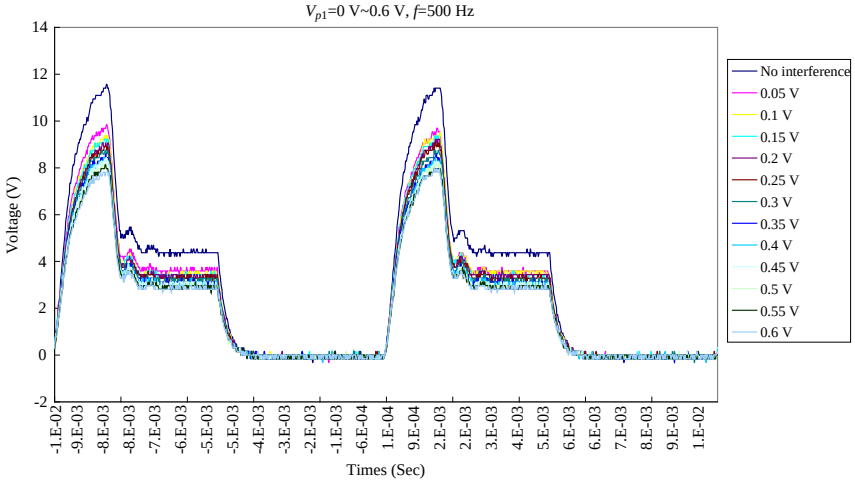

Figure 3. Effect of reverse pulse amplitude interference V_{P1} on detected voltage waveform.

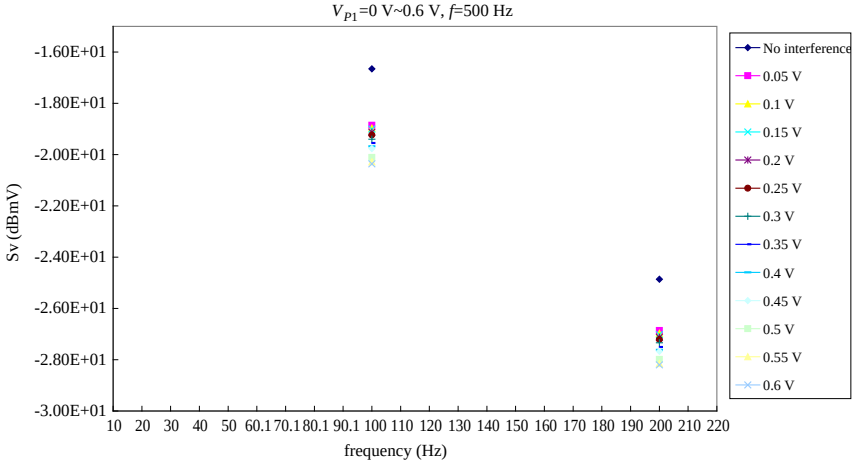

Figure 4. Effect of reverse pulse amplitude interference V_{P1} on detected light intensity spectrum.

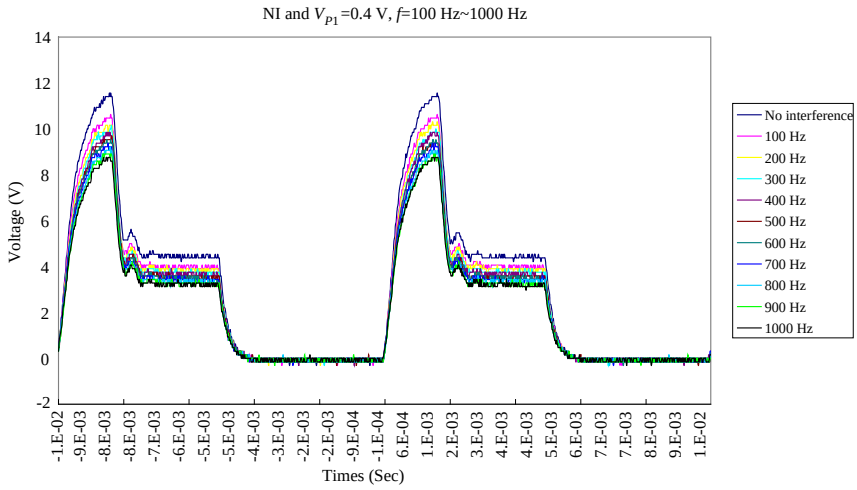

Figure 5. Effect of reverse pulse frequency interference $P1$ on detected voltage waveform.

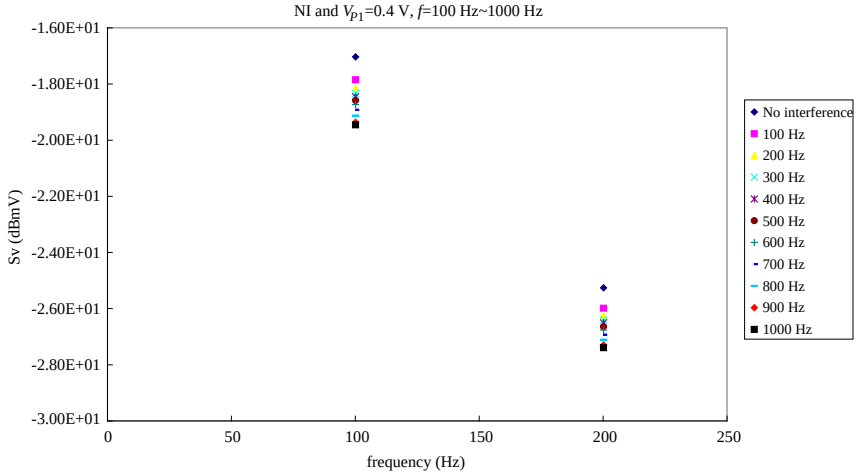

Figure 6. Effect of reverse pulse frequency interference $P1$ on detected light intensity spectrum.

4. EXPERIMENTAL RESULTS

As described in the following, the present experiments involved six different measurement modes. (a) Reverse pulse amplitude interference 1: apply a pulse wave signal with a constant frequency of $f = 500\,\text{Hz}$ and an amplitude in the range of $V_{P1} = 0\sim0.6\,\text{V}$ to points A1 and B1 of IS 1, meanwhile apply a voltage with a constant amplitude of $V_{P2} = 0.4\,\text{V}$ to points A2 and B2 of IS 2. (b) Reverse pulse frequency interference 1: apply a constant pulse amplitude $V_{P1} = 0.4\,\text{V}$ and variable pulse frequency in the range of $f = 100\,\text{Hz}\sim1000\,\text{Hz}$ to points A1 and B1 of IS 1, at same time apply a voltage with a constant amplitude of $V_{P2} = 0.4\,\text{V}$ to points A2 and B2 of IS 2. (c) Reverse pulse amplitude interference 2: apply a fixed pulse frequency of $f = 500\,\text{Hz}$ to points A2 and B2 of IS 2 and vary the pulse amplitude in the range of $V_{P2} = 0\,\text{V}\sim0.6\,\text{V}$, apply a fixed voltage amplitude of $V_{P1} = 0.4\,\text{V}$ to points A1 and B1 of IS 1. (d) Reverse pulse frequency interference 2: apply a constant pulse amplitude of $V_{P2} = 0.4\,\text{V}$ to points A2 and B2 of IS 2 and vary the pulse frequency in the range of $f = 100\,\text{Hz}\sim1000\,\text{Hz}$ apply a constant voltage amplitude of $V_{P1} = 0.4\,\text{V}$ to points A1 and B1 of IS 1. (e) Forward pulse amplitude interference 2: the measurement method is similar to method (c). (f) Forward pulse frequency interference 2: measurement is same as method (d).

(a) Reverse pulse amplitude interference 1 (apply a variable pulse wave amplitude to IS 1 with a constant frequency $f = 500\,\text{Hz}$, and apply a constant voltage $V_{P2} = 0.4\,\text{V}$ to IS 2): input pulse amplitude

$V_{P1} = 0\,\text{V}\sim0.6\,\text{V}$ applied to points A1 and B1 of IS 1 with step $\Delta V_{P1} = 0.05\,\text{V}$. The corresponding measurement results for the root mean square voltage V_{rms}, optical power, and number of photons/sec are presented in Table 1. The oscilloscope traces and spectrum analysis results are presented in Figures 3 and 4, respectively. The results show that as the amplitude of the pulsed interference voltage increases, the intensity of the detected laser beam reduces.

(b) Reverse pulse frequency interference 1 (apply a variable pulse frequency to IS1 1 with a constant pulse amplitude $V_{P1} = 0.4\,\text{V}$, and apply a constant voltage $V_{P2} = 0.4\,\text{V}$ to IS 2): pulse frequency $f = 100\,\text{Hz}\sim1000\,\text{Hz}$ applied to points A1 and B1 of IS 1 with step $\Delta f = 100\,\text{Hz}$. Table 2 presents the V_{rms} and optical power measurements. Figures 5 and 6 show the corresponding oscilloscope traces and spectrum analysis results. It is seen that the light intensity reduces as the interference pulse frequency increases.

(c) Reverse pulse amplitude interference 2: (apply a variable pulse amplitude to IS 2 with a constant pulse frequency $f = 500\,\text{Hz}$, and apply a constant voltage $V_{P1} = 0.4\,\text{V}$ to IS 1): pulse amplitude $V_{P2} = 0\,\text{V}\sim0.6\,\text{V}$ applied to points A2 and B2 of IS 2 with step $\Delta V_{P2} = 0.05\,\text{V}$. Table 3 presents the measured values of the root mean square voltage V_{rms} and optical power. Figure 7 shows the oscilloscope traces and Figure 8 shows the spectrum analysis results. It is seen that the intensity of the detected laser beam reduces as the amplitude of the interference increases.

Table 2. Effect of reverse pulse frequency interference $P1$ on laser beam voltage, optical power and photon number.

Interference frequency ($P1$)	V_{rms}	Optical power P_{PIN}	$\Delta P_{\text{PIN}} = P_x - P_{\text{NI}}$	Number of photons/sec
No interference (NI)	4.721 V	7.05 μW	0 μW	0
100 Hz	4.291 V	6.94 μW	0.11 μW	2.944E11
200 Hz	4.147 V	6.85 μW	0.20 μW	5.353E11
300 Hz	4.053 V	6.66 μW	0.39 μW	1.044E12
400 Hz	3.961 V	6.5 μW	0.55 μW	1.472E12
500 Hz	3.878 V	6.41 μW	0.64 μW	1.713E12
600 Hz	3.832 V	6.34 μW	0.71 μW	1.900E12
700 Hz	3.74 V	6.28 μW	0.77 μW	2.061E12
800 Hz	3.651 V	6.17 μW	0.88 μW	2.355E12
900 Hz	3.594 V	6.04 μW	1.01 μW	2.703E12
1000 Hz	3.512 V	5.95 μW	1.10 μW	2.944E12

Table 3. Effect of reverse pulse amplitude interference V_{P2} on laser beam voltage, optical power and photon number.

Interference amplitude (V_{P2})	V_{rms}	Optical power P_{PIN}	$\Delta P_{\text{PIN}} = P_x - P_{\text{NI}}$	Number of photons/sec
No interference (NI)	4.127 V	5.49 μW	0 μW	0
0.05 V	3.507 V	5.3 μW	0.19 μW	5.086E11
0.1 V	3.296 V	5.2 μW	0.29 μW	7.762E11
0.15 V	3.103 V	5.08 μW	0.41 μW	1.097E12
0.2 V	2.897 V	4.96 μW	0.53 μW	1.419E12
0.25 V	2.77 V	4.82 μW	0.67 μW	1.793E12
0.3 V	2.626 V	4.62 μW	0.87 μW	2.329E12
0.35 V	2.553 V	4.55 μW	0.94 μW	2.516E12
0.4 V	2.314 V	4.42 μW	1.07 μW	2.864E12
0.45 V	2.289 V	4.22 μW	1.27 μW	3.399E12
0.5 V	2.234 V	4.16 μW	1.33 μW	3.560E12
0.55 V	2.141 V	4.05 μW	1.44 μW	3.854E12
0.6 V	2.034 V	3.96 μW	1.53 μW	4.095E12

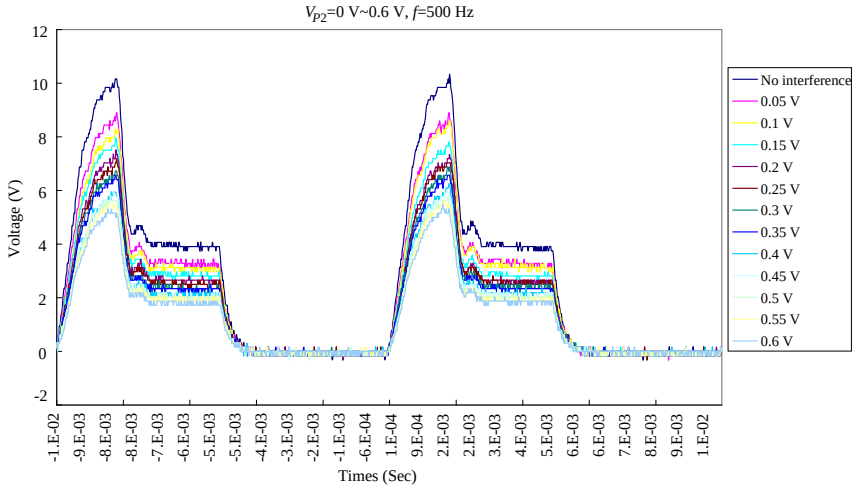

Figure 7. Effect of reverse pulse amplitude interference V_{P2} on detected voltage waveform.

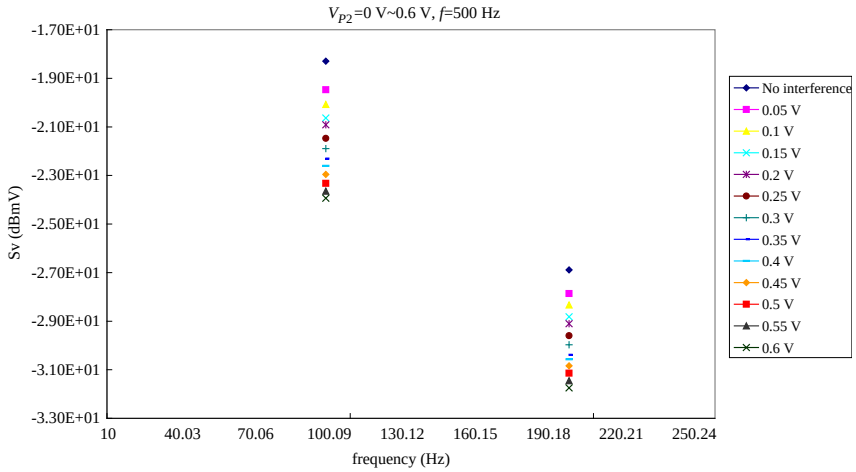

Figure 8. Effect of reverse pulse amplitude interference V_{P2} on detected light intensity spectrum.

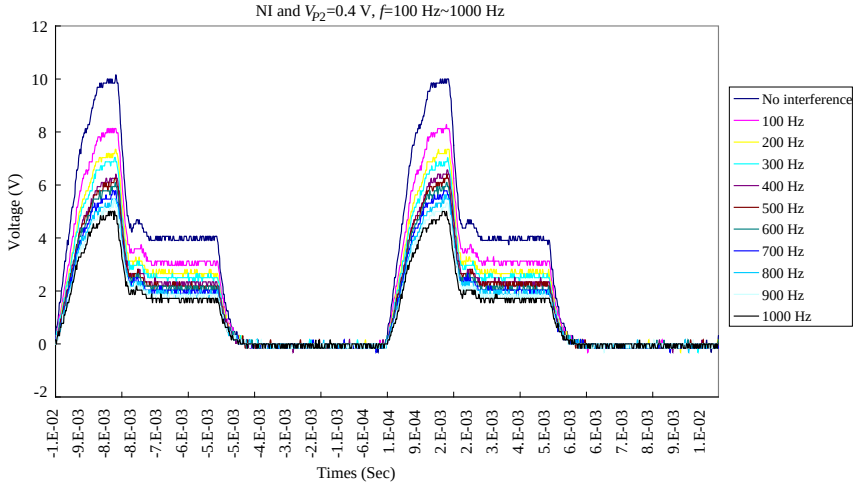

Figure 9. Effect of reverse pulse frequency interference $P2$ on detected voltage waveform.

(d) Reverse pulse frequency interference 2: (apply a variable pulse frequency to IS 2 with a constant pulse amplitude $V_{P2} = 0.4\,\mathrm{V}$, and apply a constant voltage $V_{P1} = 0.4\,\mathrm{V}$ to IS 1): pulse frequency $f = 100\,\mathrm{Hz}\sim1000\,\mathrm{Hz}$ applied to points A2 and B2 of IS 2 with step $\Delta f = 100\,\mathrm{Hz}$. Table 4 presents the

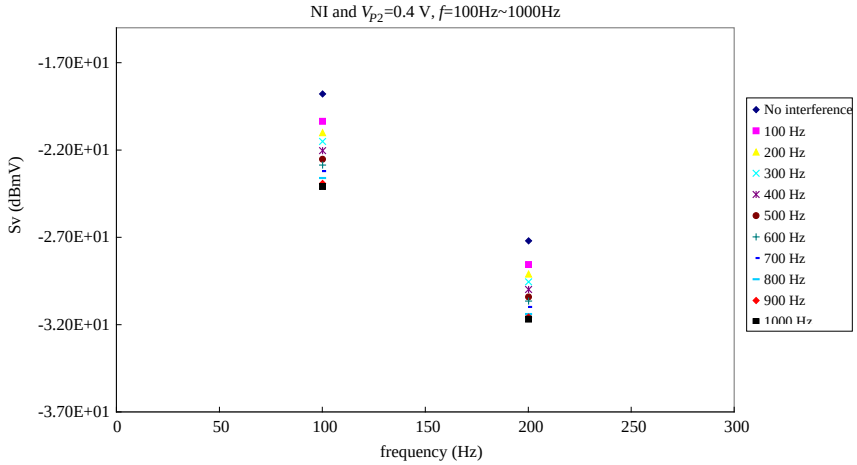

Figure 10. Effect of reverse pulse frequency interference $P2$ on detected light intensity spectrum.

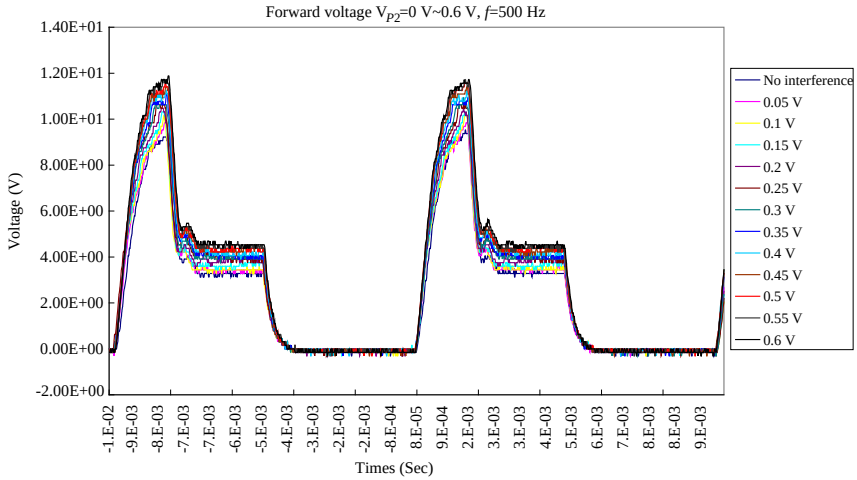

Figure 11. Effect of forward pulse amplitude interference V_{P2} on detected voltage waveform.

Table 4. Effect of reverse pulse frequency interference $P2$ on laser beam voltage, optical power and photon number.

Interference Frequency ($P2$)	V_{rms}	Optical power P_{PIN}	$\Delta\mathrm{P}_{\mathrm{PIN}} = P_x - P_{\mathrm{NI}}$	Number of photons/sec
No interference (NI)	4.174 V	5.32 μW	0 μW	0
100 Hz	3.316 V	5.12 μW	0.20 μW	5.353E11
200 Hz	2.927 V	4.96 μW	0.36 μW	9.636E11
300 Hz	2.777 V	4.88 μW	0.44 μW	1.178E12
400 Hz	2.516 V	4.79 μW	0.53 μW	1.419E12
500 Hz	2.435 V	4.72 μW	0.60 μW	1.606E12
600 Hz	2.349 V	4.62 μW	0.70 μW	1.874E12
700 Hz	2.235 V	4.46 μW	0.86 μW	2.302E12
800 Hz	2.132 V	4.35 μW	0.97 μW	2.596E12
900 Hz	2.047 V	4.22 μW	1.10 μW	2.944E12
1000 Hz	1.921 V	4.12 μW	1.20 μW	3.212E12

measurement results for the root mean square voltage V_{rms} and optical power. Figures 9 and 10 present the detected voltage waveforms and spectrum analysis results, respectively. The results show that the light intensity reduces with an increasing interference frequency.

(e) Forward pulse amplitude interference 2: (apply a variable pulse amplitude to IS 2 with a constant pulse frequency $f = 500\,\text{Hz}$, and apply a constant $V_{P1} = 0.4\,\text{V}$ to IS 1): pulse amplitude $V_{P2} = 0\,\text{V}\sim0.6\,\text{V}$ applied to points A2 and B2 of IS 2 with step $\Delta V_{P2} = 0.05\,\text{V}$. Table 5 presents the measurement results obtained for the root mean square voltage V_{rms} and optical power. Figure 11 shows the waveforms of the interfered output voltage signal. Figure 12 presents the spectrum analysis results. It is seen that as the amplitude of the interference voltage increases, the intensity of the detected light signal also increases.

(f) Forward pulse frequency interference 2: (apply a variable pulse frequency to IS 2 with a constant pulse amplitude $V_{P2} = 0.4\,\text{V}$, and apply a constant voltage $V_{P1} = 0.4\,\text{V}$ to IS 2): pulse frequency $f = 100\,\text{Hz}\sim1000\,\text{Hz}$ applied to points A2 and B2 of IS 2 with step $\Delta f = 100\,\text{Hz}$. Table 6 shows the measured values of the root mean square voltage V_{rms} and optical power. Figures 13 and 14 show the detected output voltage waveforms and the spectrum analysis results, respectively. The results show that the intensity of the detected light signal increases with an increasing interference frequency.

Table 5. Effect of forward pulse amplitude interference V_{P2} on laser beam voltage, optical power and photon number.

Interference amplitude (V_{P2})	V_{rms}	Optical power P_{PIN}	$\Delta P_{\text{PIN}} = P_x - P_{\text{NI}}$	Number of photons/sec
No interference (NI)	3.677 V	4.22 μW	0 μW	0
0.05 V	3.757 V	4.32 μW	0.10 μW	2.677E11
0.1 V	3.77 V	4.46 μW	0.24 μW	6.424E11
0.15 V	3.929 V	4.55 μW	0.33 μW	8.833E11
0.2 V	4.061 V	4.62 μW	0.40 μW	1.071E12
0.25 V	4.266 V	4.72 μW	0.50 μW	1.338E12
0.3 V	4.3 V	4.95 μW	0.73 μW	1.954E12
0.35 V	4.428 V	5.02 μW	0.80 μW	2.141E12
0.4 V	4.549 V	5.24 μW	1.02 μW	2.730E12
0.45 V	4.653 V	5.36 μW	1.14 μW	3.051E12
0.5 V	4.719 V	5.42 μW	1.20 μW	3.212E12
0.55 V	4.832 V	5.66 μW	1.44 μW	3.854E12
0.6 V	4.909 V	5.72 μW	1.50 μW	4.015E12

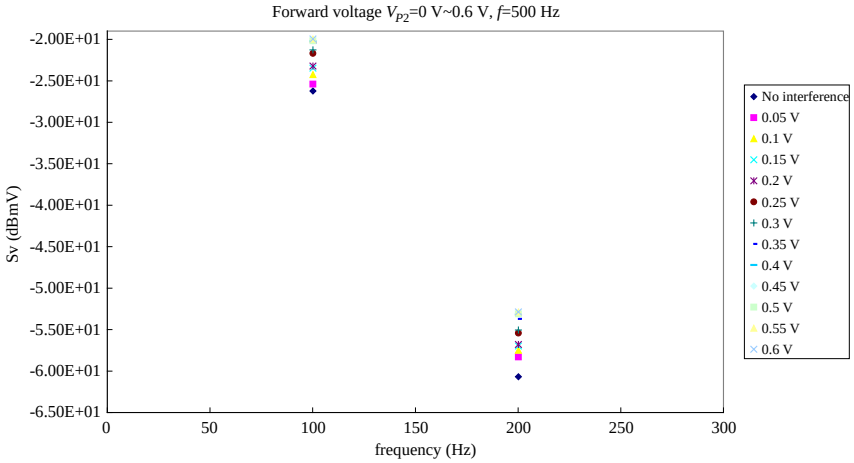

Figure 12. Effect of forward pulse amplitude interference V_{P1} on detected light intensity spectrum.

Table 6. Effect of forward pulse frequency interference $P2$ on laser beam voltage, optical power and photon number.

Interference frequency ($P2$)	$V_{\rm rms}$	Optical power $P_{\rm PIN}$	$\Delta P_{\rm PIN} = P_x - P_{\rm NI}$	Number of photons/sec
No interference (NI)	3.455 V	3.5 μW	0 μW	0
100 Hz	3.522 V	3.76 μW	0.11 μW	2.944E11
200 Hz	3.555 V	3.86 μW	0.20 μW	5.353E11
300 Hz	3.584 V	4.12 μW	0.39 μW	1.044E12
400 Hz	3.652 V	4.22 μW	0.55 μW	1.472E12
500 Hz	3.773 V	4.35 μW	0.64 μW	1.713E12
600 Hz	3.804 V	4.46 μW	0.71 μW	1.900E12
700 Hz	3.997 V	4.62 μW	0.77 μW	2.061E12
800 Hz	4.072 V	4.72 μW	0.88 μW	2.355E12
900 Hz	4.197 V	4.79 μW	1.01 μW	2.703E12
1000 Hz	4.214 V	4.88 μW	1.10 μW	2.944E12

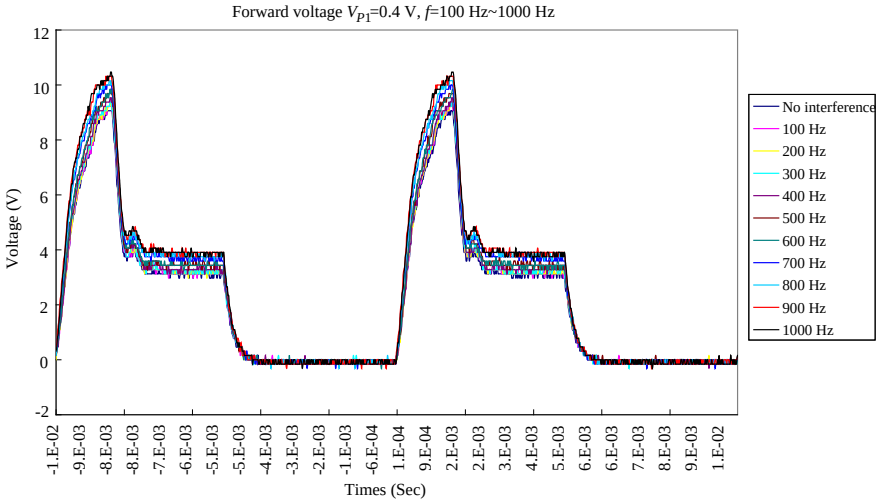

Figure 13. Effect of forward pulse frequency interference $P2$ on detected voltage waveform.

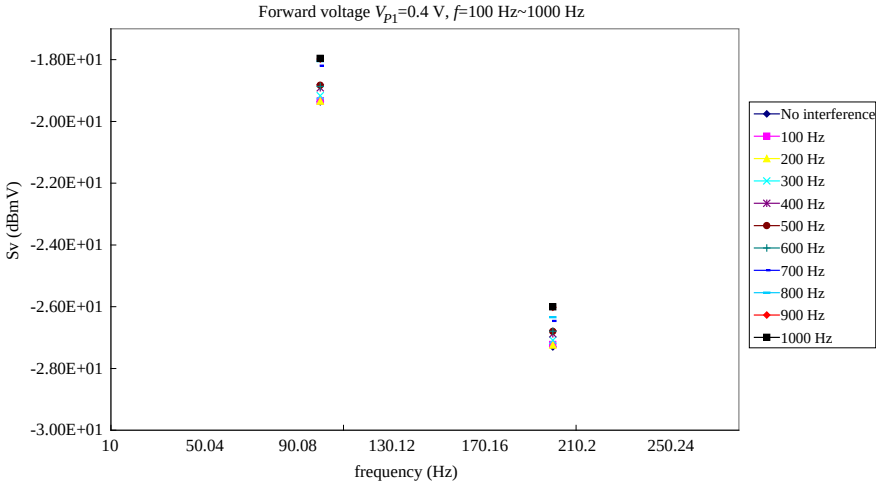

Figure 14. Effect of forward pulse frequency interference $P2$ on detected light intensity spectrum.

Table 7. Measured values of ΔP_{PIN} and ΔV_{rms} for IS 1 and IS 2 under reverse EMD conditions.

Max. ΔP_{PIN} (ΔV_{rms}) in cases a and b (reverse IS 1).		Max. ΔP_{PIN} (ΔV_{rms}) in cases c and d (reverse IS 2).	
a	b	c	d
1.28 μW (1.527 V)	1.10 μW (1.209 V)	1.53 μW (2.093 V)	1.20 μW (2.253 V)

Note: $\Delta P_{\mathrm{PIN}} = P_{\mathrm{No\ interference}} - P_{0.6\,\mathrm{V}}$, $\Delta V_{\mathrm{rms}} = V_{\mathrm{rms\ No\ interference}} - V_{\mathrm{rms}\ 0.6\,\mathrm{V}}$.

Table 7 summarizes the values of ΔP_{PIN} and ΔV_{rms} for cases (a) and (b), corresponding to IS 1, cases (c) and (d), corresponding to IS 2. The results show that the impact of EMD on the laser beam power and voltage increases as the dispersion of the laser beam (i.e., the distance from the laser source) increases.

By the above tables, the electromagnetic field acts in the opposite direction to that of the laser beam, the intensity and optical power of the detected signal decrease with an increasing interference frequency or amplitude. By contrast, when the electromagnetic field acts in the same direction as that of the laser beam, the intensity and optical power increase with an increasing interference frequency or amplitude. In addition, the Table 7 is shown that the effect of EMD on the intensity of the laser beam increases with an increasing laser beam dispersion.

5. CONCLUSION

The results have shown that for the case in which the electromagnetic field acts in the opposite direction to that of the laser beam, the detected light intensity and optical power decrease as the amplitude and frequency of the interference voltage increase. By contrast, when the electromagnetic field acts in the same direction as the laser beam, the light intensity and optical power both increase with an increasing interference amplitude and frequency. In addition, the results have shown that as the dispersion of the laser beam increases (i.e., the distance from the laser source increases), the effects of EMD become increasingly pronounced. In general, the results presented in this study confirm that EMD has an adverse effect not only on the performance of electrical and electronic circuits, but also on the optical performance of laser systems. Thus, in designing laser systems in which the output power and optical density are an important concern, the need for effective EMD shielding strategies must be carefully considered.

ACKNOWLEDGMENT

The author wishes to acknowledge the invaluable assistance provided by Tsair-Jan Hwang throughout the course of this study.

REFERENCES

1. Dincer, F., O. Akgol, M. Karaaslan, E. Unal, and C. Sabah, "Polarization angle independent perfect metamaterial absorbers for solar cell applications in the microwave, infrared, and visible regime," *Progress In Electromagnetics Research*, Vol. 144, 93–101, 2014.
2. Wefky, A., F. Espinosa, L. de Santiago, A. Gardel, P. Revenga, and M. Martinez, "Modeling radiated electromagnetic emissions of electric motorcycles in terms of driving profile using MLP neural networks," *Progress In Electromagnetics Research*, Vol. 135, 231–244, 2013.
3. Santorelli, A., M. Chudzik, E. Kirshin, E. Porter, A. Lujambio, I. Arnedo, M. Popovic, and J. D. Schwartz, "Experimental demonstration of pulse shaping for time-domain microwave breast imaging," *Progress In Electromagnetics Research*, Vol. 133, 309–329, 2013.
4. Liu, C.-C. and C.-J. Wu, "Near infrared filtering properties in photonic crystal containing extrinsic and dispersive semiconductor defect," *Progress In Electromagnetics Research*, Vol. 137, 359–370, 2013.

5. Ding, D. G., F. Luo, and W. C. Zhou, "Effects of thermal oxidation on electromagnetic interference shielding properties of SiC_f/SiC composites," *Ceramics International*, Vol. 39, 4281–4286, 2013.
6. Joseph, N., S. K. Singh, R. K. Sirugudu, V. R. K. Murthy, S. Ananthakumar, and M. T. Sebastian, "Effect of silver incorporation into PVDF-barium titanate composites for EMI shielding applications," *Materials Research Bulletin*, Vol. 48, 1681–1687, 2013.
7. Moon, Y. E., J. Yun, and H. I. Kim, "Synergetic improvement in electromagnetic interference shielding characteristics of polyaniline-coated graphite oxide/γ-Fe_2O_3/$BaTiO_3$ nanocomposites," *Journal of Industrial and Engineering Chemistry*, Vol. 19, 493–497, 2013.
8. Chen, J. and Z. Du, "Device simulation studies on latch-up effects in CMOS inverters induced by microwave pulse," *Microelectronics Reliability*, Vol. 53, 371–378, 2013.
9. Tlig, M., J. Ben Hadj Slama, and M. A. Belaid, "Conducted and radiated EMI evolution of power RF N-LDMOS after accelerated ageing tests," *Microelectronics Reliability*, Vol. 53, 1793–1797, 2013.
10. Kim, H. R., K. Fujimori, B. S. Kim, and I. S. Kim, "Lightweight nanofibrous EMI shielding nanowebs prepared by electrospinning and metallization," *Composites Science and Technology*, Vol. 72, 1233–1239, 2013.
11. Kaur, A., Ishpal, and S. K. Dhawan, "Tuning of EMI shielding properties of polypyrrole nanoparticles with surfactant concentration," *Synthetic Metals*, Vol. 162, 1471–1477, 2012.
12. Groos, G., "Characterisation method for chip card ESD events causing terminal failures," *Microelectronics Reliability*, Vol. 52, 2005–2009, 2012.
13. Jang, C. K., J. H. Park, and J. Y. Jaung, "MWNT/PEG grafted nanocomposites and an analysis of their EMI shielding properties," *Materials Research Bulletin*, Vol. 47, 2767–2771, 2012.
14. Guo, H., H. Wu, B. Zhang, and Z. Li, "Research on periodic switching frequency modulation for conducted EMI suppressing in power converter," *Microelectronics Journal*, Vol. 42, 415–421, 2011.
15. Guo, H., H. Wu, B. Zhang, and Z. Li, "A novel spread-spectrum clock generator for suppressing conducted EMI in switching power supply," *Microelectronics Journal*, Vol. 41, 93–98, 2010.
16. Tsai, H. C., "Investigation into time- and frequency-domain emi-induced noise in bistable multivibrator," *Progress In Electromagnetics Research*, Vol. 100, 327–349, 2010.
17. Wang, W., Y. Huang, X. Duan, Y. Zhou, J. Guo, and X. Ren, "Monolithically integrated tunable dual-wavelength photodetector with flat-top response," *Optics Communications*, Vol. 285, 638–644, 2012.
18. Ramesh, R., M. Madheswaran, and K. Kannan, "Physical noise model of a uniformly doped nanoscale FinFET photodetector," *Optik — International Journal for Light and Electron Optics*, Vol. 123, 1087–1094, 2012.
19. Pavel, A. A., N. E. Islam, A. K. Sharma, C. S. Mayberry, and S. L. Lucero, "Minimizing reflection and focussing of incident wave to enhance energy deposition in photodetector's active region," *Progress In Electromagnetics Research*, Vol. 65, 71–80, 2006.
20. Cheng, D. K., *Field and Wave Electromagnetics,* 2nd edition, 231–232, Addison-Wesley Publishing Company, USA, 1989.
21. Cheng, D. K., *Field and Wave Electromagnetics,* 2nd edition, 252–280, Addison-Wesley Publishing Company, USA, 1989.
22. Giancoli, D. C., *Physics for Scientists & Engineers,* 3rd edition, 952–961, Prentice-Hall International Limited, London, UK, 2000.